Inorg. Chem. **2007**, *46*, 10071–10078

cis-Dichloro-bis(4,4′-dicarboxy-2,2-bipyridine)osmium(II)-Modified Optically Transparent Electrodes: Application as Cathodes in Stacked Dye-Sensitized Solar Cells

Michael J. Scott,[†] Jeremy J. Nelson,[†] Stefano Caramori,[‡] Carlo A. Bignozzi,*[,‡] and C. Michael Elliott*[,†]

Department of Chemistry, Colorado State University, Fort Collins, Colorado 80523-1872 USA, Dipartimento di Chimica, Università di Ferrara, Via Luigi Borsari 46, 44100 Ferrara, Italy

Received April 13, 2007

An optically transparent cathode was developed for use in dye-sensitized solar cells. Fluorine-doped tin oxide conducting glass modified with a monolayer of *cis*-dichloro-bis(4,4′-dicarboxy-2,2′-bipyridine)osmium(II) efficiently reduces the oxidized form of the redox mediator. This transparent cathode transmits light that is not absorbed by the dyed TiO_2; consequently, more than one cell can operate in optical tandem (i.e., stacked). Two types of stacked cells are considered: one where both photoanodes are dyed with the same dye and one where the photoanodes are dyed with different, spectrally complementary dyes. Overall behavior of these tandem cells is compared with single-cell analogs.

Introduction

Since the present-day incarnation of the dye-sensitized solar cell (DSSC) was described by Grätzel and co-workers,[1] much effort has focused on maximizing the energy-conversion efficiency and device lifetime while minimizing production costs and environmental impact. Energy conversion in a DSSC is characterized by three processes: (1) Photooxidation of the sensitizing dye via injection of electrons into the conduction band of, typically, nanocrystalline TiO_2, (2) reduction of the oxidized dye by a redox mediator in solution, and (3) reduction of the oxidized mediator at the cathode.

$$D^* \rightarrow D^+ + e^-_{cb} \quad (1)$$

$$D^+ + R \rightarrow D + R^+ \quad (2)$$

$$R^+ + e^-_{cathode} \rightarrow R \quad (3)$$

These processes efficiently separate charge and confine the electrons to the solid semiconductor phase and the holes to the liquid electrolyte phase. The predominant processes that negatively influence cell efficiencies are: (4) recombination of the photoinjected electron with oxidized dye, or (5) with oxidized mediator.

$$D^+ + e^-_{cb} \rightarrow D \quad (4)$$

$$R^+ + e^-_{cb} \rightarrow R \quad (5)$$

The defining feature of the present-day DSSC is the extremely high surface area mesoporous photoanode fabricated from nanometer-sized TiO_2 crystals. The mesoporous semiconductor is deposited as a thin layer (usually less than 10 μm thick) on a transparent conducting substrate, resulting in a 3D structure that has an actual surface area ca. 1000 times greater than the apparent surface area. After dying, the pores of this 3D structure are typically filled with mediator electrolyte solution. Within the resulting bicontinuous phase, the domains are small (i.e., less than ca. 50 nm), thus no macroscopic electric field can be sustained in the TiO_2 because of screening by the electrolyte.[2,3] For this reason, photoinjected electrons travel through the porous

* To whom correspondence should be addressed. E-mail: elliott@lamar.colostate.edu.
[†] Colorado State University.
[‡] Università di Ferrara.

(1) Oregan, B.; Grätzel, M. A Low-Cost, High-Efficiency Solar-Cell Based on Dye-Sensitized Colloidal TiO_2 Films. *Nature* **1991**, *353* (6346), 737−740.
(2) Bisquert, J.; Garcia-Belmonte, G.; Fabregat-Santiago, F. Modelling the Electric Potential Distribution in the Dark in Nanoporous Semiconductor Electrodes. *J. Solid State Electrochem.* **1999**, *3* (6), 337−347.
(3) Rothenberger, G.; Fitzmaurice, D.; Grätzel, M.; Spectroscopy of Conduction-Band Electrons in Transparent Metal-Oxide Semiconductor-Films - Optical Determination of the Flat-Band Potential of Colloidal Titanium-Dioxide Films. *J. Phys. Chem.* **1992**, *96* (14), 5983−5986.

10.1021/ic700709k CCC: $37.00
Published on Web 11/02/2007

TiO_2 structure to the underlying conducting glass substrate via a diffusional random walk pathway. Along this course, electrons temporarily reside in trap states for periods of time dependent on the depth of the trap.[4] Thus the electron can be thought of as moving (diffusing) randomly (i.e., toward or away from the collector electrode) from trap to trap. Because of this diffusional motion, doubling the distance between the collector and the photo-oxidized dye site quadruples the electron's residence time in the TiO_2. Therefore, the probability that the electron will recombine with a photo-oxidized dye molecule or react with the oxidized mediator is also approximately quadrupled. The net consequence is that the photocurrent does not scale linearly with increased light absorption for a thicker TiO_2 layer,[5] provided that the thickness of the layer is similar to or greater than the average electron diffusion length.

The iodide (I^-/I_3^-) redox couple is by far the dominant mediator system used in DSSCs. This prevalence is for two kinetic reasons: first, the reduction of the photo-oxidized dye by I^- (R in the above reactions) is very fast, and second, the reaction of injected electrons with I_3^- (R^+ in the above reactions) is very slow.[6] Montanari et al. have shown that, for DSSCs having photoanodes that incorporate the so-called N3 dye (*cis*-di(isothiocyanato)-bis(4,4′-dicarboxy-2,2′-bipyridine)ruthenium(II)), and mediated by I^-/I_3^-, the reduction of the photo-oxidized sensitizing dye by I^- is sufficiently fast that the predominant recombination reaction is that of the conduction-band electron with the oxidized form of the mediator (reaction 5 above).[7] However, transient laser spectroscopy experiments completed in our respective laboratories[8,9] and results published by Nusbaumer et al.[10] have shown that in cobalt-mediated DSSCs, reduction of the photo-oxidized sensitizing dye by cobalt(II) is not as efficient as that observed in I^-/I_3^--mediated DSSCs. For this reason, the recombination reaction of the conduction-band electron with the photo-oxidized dye, in reaction 4 above, cannot be dismissed when considering DSSCs employing alternative redox mediator systems.

Unfortunately, the I^-/I_3^- redox couple has several negative features within the context of its application as a DSSC mediator: I_2 in equilibrium with I_3^- is volatile, cathodes must be constructed from platinum-group metals, I_3^- is darkly colored and absorbs visible light, and the redox potential of the I^-/I_3^- couple is more negative than optimum (for use with standard dyes, at least) − to name a few. Consequently, there is inherent interest in the discovery of redox couples that avoid some or all of these problems while still functioning efficiently as mediators in the DSSC. Several years ago, we reported that certain polypyridine complexes of cobalt function as reasonable DSSC mediators exhibiting relative efficiencies greater than 80% of a comparable I^-/I_3^--mediated cell, without most of the undesirable properties of the I^-/I_3^- couple.[11] Of the polypyridine cobalt mediators studied thus far, tris(4,4′-di-*tert*-butyl-2,2′-bipyridine)cobalt(II/III) ($Co(DTB)_3^{2+/3+}$) is one of the best in our hands.

As mentioned above, increasing the thickness of the absorbing-dyed TiO_2 layer does not result in a proportional increase in photocurrent. The I^-/I_3^- couple imposes restrictions on strategies that might be employed to deal with this and other issues. When unbridled from these restrictions by employing the $Co(DTB)_3^{2+/3+}$ mediator system, a number of otherwise unavailable options present themselves. For example, one possible way to circumvent the problem associated with increasing the photoanode thickness is to run multiple cells in optical tandem (i.e., stack them). Doing this requires, however, that the cathode be optically transparent.

Whereas many electrode materials function at least adequately as cathodes in $Co(DTB)_3^{2+/3+}$-mediated cells (gold, carbon, platinum); they are opaque. In contrast, native (unmodified) transparent indium-doped tin oxide (ITO) and fluorine-doped tin oxide (FTO) electrodes function extremely poorly as cathodes in $Co(DTB)_3^{2+/3+}$-mediated cells.[11] However, when these optically transparent conducting oxides (collectively TCO) are modified by adsorbing certain metal complexes on their surfaces, they become catalytic to the oxidation of $Co(DTB)_3^{2+}$.[12] Moreover, when the $E_{1/2}$ of the adsorbed catalyst coincides with that of $Co(DTB)_3^{2+/3+}$, both the oxidation and reduction of the $Co(DTB)_3^{2+/3+}$ are catalyzed resulting in quasi-reversible voltammetry. An example of such a catalyst is *cis*-dichloro-bis(4,4′-dicarboxylic acid-2,2′-bipyridine)osmium(II) ($Os(dcb)_2Cl_2$).

In the following, we describe studies of stacked DSSCs of two types, each employing ($Os(dcb)_2Cl_2$)-modified transparent FTO cathodes. In the first series of investigations, we consider stacked cells employing only photoanodes dyed with the standard N3 dye.[13] In the second, we consider stacked cells employing an N3-dyed anode stacked with an anode dyed with a dicarboxylated cyanine dye.[5] The cyanine

(4) Nelson, J. Continuous-Time Random-Walk Model of Electron Transport in Nanocrystalline TiO_2 Electrodes. *Phys. Rev. B* **1999**, *59* (23), 15374−15380.

(5) Ehret, A.; Stuhl, L.; Spitler, M. T.; Spectral Sensitization of TiO_2 Nanocrystalline Electrodes with Aggregated Cyanine Dyes. *J. Phys. Chem. B* **2001**, *105* (41), 9960−9965.

(6) Gregg, B. A.; Pichot, F.; Ferrere, S.; Fields, C. L. Interfacial Recombination Processes in Dye-Sensitized Solar Cells and Methods to Passivate the Interfaces. *J. Phys. Chem. B* **2001**, *105* (7), 1422−1429.

(7) Montanari, I.; Nelson, J.; Durrant, J. R. Iodide Electron Transfer Kinetics in Dye-Sensitized Nanocrystalline TiO_2 Films. *J. Phys. Chem. B* **2002**, *106* (47), 12203−12210.

(8) Cazzanti, S.; Caramori, S.; Argazzi, R.; Elliott, C. M.; Bignozzi, C. A. Efficient Non-Corrosive Electron-Transfer Mediator Mixtures for Dye-Sensitized Solar Cells. *J. Am. Chem. Soc.* **2006**, *128* (31), 9996−9997.

(9) Scott, M. J.; Elliott, C. M. Unpublished results.

(10) Nusbaumer, H.; Moser, J. E.; Zakeeruddin, S. M.; Nazeeruddin, M. K.; Grätzel, M. $Co^{II}(dbbip)_2^{2+}$ Complex Rivals Tri-Iodide/Iodide Redox Mediator in Dye-Sensitized Photovoltaic Cells. *J. Phys. Chem. B* **2001**, *105* (43), 10461−10464.

(11) Sapp, S. A.; Elliott, C. M.; Contado, C.; Caramori, S.; Bignozzi, C. A. Substituted Polypyridine Complexes of Cobalt(II/III) as Efficient Electron-Transfer Mediators in Dye-Sensitized Solar Cells. *J. Am. Chem. Soc.* **2002**, *124* (37), 11215−11222.

(12) Elliott, C. M.; Caramori, S.; Bignozzi, C. A. Indium Tin Oxide Electrodes Modified with Tris(2,2′-bipyridine-4,4′-dicarboxylic Acid) Iron(II) and the Catalytic Oxidation of Tris(4,4′-di-tert-butyl-2,2′-bipyridine) Cobalt(II). *Langmuir* **2005**, *21* (7), 3022−3027.

(13) Nazeeruddin, M. K.; Kay, A.; Rodicio, I.; Humphry-Baker, R.; Mueller, E.; Liska, P.; Vlachopoulos, N.; Grätzel, M. Conversion of Light to Electricity by cis-X_2-bis(2,2′-Bipyridyl-4,4′-dicarboxylate)ruthenium(II) Charge-Transfer Sensitizers (X = Cl^-, Br^-, I^-, CN^-, and SCN^-) on Nanocrystalline Titanium Dioxide Electrodes. *J. Am. Chem. Soc.* **1993**, *115* (14), 6382−90.

dye, R8, has a spectrum complementary to that of N3 and thus has the potential to capture a larger portion of the long-wavelength spectrum.

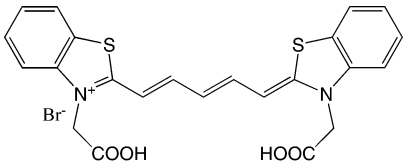

R8

Experimental Section

Materials. Cells used in this work utilized photoanodes consisting of thin layers of dyed TiO_2 deposited on FTO conducting glass (vide infra). The cathodes were either gold deposited on FTO-coated glass or catalyst-modified FTO (vide infra). Unless otherwise specified, all of the chemicals were purchased from Aldrich and used as received. The mediator solutions are 0.15 M $[Co(DTB)_3](ClO_4)_2$, 0.015 M nitrosonium tetrafluoroborate, 0.2 M 4-*tert*-butylpyridine, and 0.2 M lithium trifluoromethanesulfonate in γ-butyrolactone. Addition of $NOBF_4$ stoichiometrically oxidized the $Co(DTB)_3^{2+}$ to $Co(DTB)_3^{3+}$, resulting in a 10% oxidized-mediator solution. γ-Butyrolactone was chosen for its low vapor pressure and relatively low viscosity. Preparation of $[Co(DTB)_3](ClO_4)_2$ was completed as previously described.[11] N3 dye (*cis*-di(isothiocyanato)-bis(4,4′-dicarboxy-2,2′-bipyridine)ruthenium(II)) was synthesized using a modified literature procedure.[13]

Cell performance was evaluated by assembling a cell and measuring its current output when exposed to simulated sunlight. The photoanode and cathode were clamped together with a thin layer of redox mediator between them in a custom cell holder with a 0.4 cm^2 optical aperture. Electrical leads were connected, and the cell was illuminated with a 100 W xenon arc lamp calibrated to 100 mW cm^{-2} with a Molectron PowerMax 500A power meter. A 400 nm cutoff filter was placed between the lamp and the cell to prevent direct excitation of the TiO_2 semiconductor. Output current was measured by a Keithley Sourcemeter run by a LabView virtual instrument while the potential was scanned from 700 to −100 mV at 50 mV s^{-1}. The resulting current−voltage curves were assessed on the basis of open-circuit voltage (V_{oc}), short-circuit current density (J_{sc}), fill factor (FF), and efficiency (η) (determined by dividing the power at the maximum-power point by the incident-light power, 100 mW cm^{-2}).

To compare the light-absorbing ability of the dyed TiO_2 layers, UV−vis spectra were recorded with a HP 8452A diode array spectrometer. The dyed photoanodes were held to the instrument sample holder with double-sided tape. A clean piece of FTO substrate was used as a blank, and several positions on the photoanode were averaged for each spectrum.

Photoaction spectra, incident photon to current conversion efficiency versus wavelength, were acquired by assembling a cell in the path of a 75 W Tungsten lamp coupled to a Jarrel Ashe 0.25 m monochromator. The wavelength was scanned from 800 to 400 nm while the short circuit current was recorded by a PAR 174 polarographic analyzer linked to a computerized control and data-acquisition system.[14]

Cyclic voltammetry (CV) was used to compare the osmium-modified and gold electrodes' ability to catalyze the reduction of $Co(DTB)_3^{3+}$. A standard three-electrode cell was used with a BAS 100B Potentiostat-Galvanostat run by BAS 100W software on a personal computer. Tetraethylammonium perchlorate (0.1 M in acetonitrile) was the supporting electrolyte, and the concentration of $[Co(DTB)_3](ClO_4)_2$ was ca. 0.1 mM. A sodium saturated calomel electrode reference and a platinum-mesh counter electrode were employed. For working electrode comparisons, the electrodes were all 0.5 cm^2 and either ITO, FTO, (unmodified or osmium-modified as indicated), or gold. Electrochemical data are reported relative to ferrocene.

Electrode Preparation. Dyed Photoanodes. A thin layer of nanocrystalline TiO_2 (Solaronix) was deposited using the doctor blade technique onto FTO conducting glass.[15] Titania layers attained using a single strip of 3M Scotch Tape as a spacer will be termed "one scotch" layers. Thinner layers, termed "half scotch" were attained using stretched Parafilm as a spacer. The Parafilm was carefully and evenly stretched to 8 times its original length. This resulted in a 30 μm thick spacer (compared to 70 μm for the tape). After the applied TiO_2 layer dried in air, the coated glass was baked at 450 °C for 1 h. After cooling to room temperature, a 0.2 M aqueous solution of $TiCl_4$ was applied to the TiO_2 layer and left overnight in a high-humidity chamber.[13] After being rinsed with deionized water and dried in a nitrogen stream, the photoanode was refired at 450 °C for 1 h and then allowed to cool to 120 °C. At this point, photoanodes were placed in a saturated dye solution in dry ethanol and stored in the dark for 12−18 h to allow for dye adsorption. The dye-sensitized photoanodes were rinsed with ethanol to remove any excess dye and dried in a nitrogen stream. The thickness of deposited TiO_2 layers was determined with a Datatek Profilometer. Half scotch layers were 2.4(± 0.1) μm thick, and one scotch layers were 4.4(± 0.1) μm thick.

Patterned Electrodes. Patterned gold, FTO, and ITO electrodes, all with an area of 0.5 cm^2, were used in CV. Gold electrodes used as DSSC cathodes and as stock for patterned CV electrodes were prepared by depositing 200 nm of gold over a 15 nm layer of chromium on FTO glass in a vacuum deposition chamber. Patterned electrodes were fabricated using photolithography; small rectangles (ca. 1 × 2 cm^2) of the gold-coated FTO, bare FTO, and bare ITO were vigorously cleaned and coated with a layer of Photoresist AZ 1512 (Kodak). For the patterned ITO electrodes, the layer of ITO not covered by photoresist was removed by immersing the electrode in a dilute aqua regia solution (45% HCl, 5% HNO_3, 50% deionized H_2O) for 15−20 min.[12] For the patterned FTO electrodes, a slurry of zinc powder (6−9 μm) in deionized water was spread on the FTO-coated glass before immersing in concentrated HCl for 20−30 s. The solution bubbled vigorously as H_2 was produced, reducing the tin(IV) to tin metal, which dissolved in the acid. For the patterned gold electrodes, the gold layer was removed in the dilute aqua regia solution before the FTO layer was removed by the Zn/HCl reaction. When the two-probe resistance measured between points separated by ca. 0.5 cm was greater than 20 MΩ, the removal was considered complete, and the protective photoresist was rinsed off with acetone.

Transparent Cathodes. *cis*-Dichloro-bis(4,4′-dicarboxylic acid-2,2′-bipyridine)osmium(II) ($Os(dcb)_2Cl_2$) was synthesized using a modified literature procedure.[16] Transparent conducting oxide electrodes modified with $Os(dcb)_2Cl_2$ were prepared by first soaking TCO electrodes in a KOH base bath for 20 min. The electrodes

(14) Fillinger, A.; Soltz, D.; Parkinson, B. A. Dye Sensitization of Natural Anatase Crystals with a Ruthenium-Based Dye. *J. Electrochem. Soc.* **2002**, *149* (9), A1146−A1156.

(15) Zaban, A.; Ferrere, S.; Sprague, J.; Gregg, B. A. pH-Dependent, Redox Potential Induced in a Sensitizing Dye by Adsorption onto TiO_2. *J. Phys. Chem. B* **1997**, *101* (1), 55−57.

(16) Buckingham, D. A.; Dwyer, F. P.; Goodwin, H. A.; Sargeson, A. M. Mono- and Bis-(2,2-bipyridine) and (1,10-Phenanthroline) Chelates of Ruthenium and Osmium IV. Bis Chelates of Bivalent and Tervalent Osmium. *Aust. J. Chem.* **1964**, *17* (3), 325−336.

were rinsed with tap water, deionized water, and 95% ethanol before drying under a nitrogen stream. The electrodes were then placed in a solution of Alconox in deionized water in an ultrasonic cleaner for 15 min, rinsed, dried, and then sonicated in electronics-grade isopropanol for 15 min. Following this treatment, the dried electrodes were transferred to a plasma cleaner and exposed to an air plasma for 45 min.[17] A monolayer of $Os(dcb)_2Cl_2$ was adsorbed onto the TCO surface by soaking the electrode overnight in a dry-ethanol solution of $Os(dcb)_2Cl_2$. The $Os(dcb)_2Cl_2$-modified electrodes were then rinsed with dry ethanol and dried under a nitrogen stream.

Split Photoanodes. For three-electrode photocell measurements, a split photoanode was fabricated using a procedure similar to that used to prepare regular photoanodes. Prior to treatment with 0.2 M aqueous $TiCl_4$, a linear groove roughly bisecting the photoanode area was cut through the TiO_2 and FTO layers using a small grinding wheel mounted in a Dremel tool. The resistance across the resulting gap was consistently greater than 350 MΩ. Following $TiCl_4$ treatment, the photoanode was rinsed, baked, and dyed according to the standard procedure (vide supra). Once the cell was assembled, one-half of the split anode functioned as a conventional photoanode while the other served as the reference in the three-electrode configuration. As no current is drawn from the reference half, the electrode should maintain a constant potential at V_{oc} under illumination. Typically, a slight difference in V_{oc} existed for the two photoanodes (less than ca. 25 mV) most likely due to such factors as slight variations in surface dye concentration, illumination intensity, etc.

Current−voltage curves were measured using a locally constructed operational amplifier potentiostat circuit designed to allow the potential difference between the cathode and the photoanode to be controlled while monitoring the potential of the reference relative to the photoanode (held at instrument ground). The potential of the cathode relative to the reference can thus be determined by difference. A PAR Model 175 Universal Programmer was used to control the potential across the cell. Output signals (cathode potential, reference potential, and current) were recorded simultaneously using a computer equipped with a NI DAQ board, BNC connector box, and *LabView* software.

Results and Discussion

Osmium-Modified Transparent Cathodes. As stated in the introduction, many materials function as cathodes in $Co(DTB)_3^{2+/3+}$-mediated DSSCs; however, bare TCO electrodes do not. This is not unexpected because, were heterogeneous electron transfer between the $Co(DTB)_3^{2+/3+}$ couple and FTO rapid, recombination between photoinjected electrons in the FTO conduction band and $Co(DTB)_3^{3+}$ would also be fast. In an earlier study, we demonstrated that, in contrast to bare TCO substrates, FTO and ITO electrodes modified by irreversibly adsorbing a monolayer of $Fe(dcb)_3^{2+}$ very efficiently oxidized $Co(DTB)_3^{2+}$.[12] In this case, the oxidized $Fe(dcb)_3^{3+}$ surface species catalyzes the oxidation of $Co(DTB)_3^{2+}$ via an EC′ (i.e., surface catalytic) mechanism. The $E_{1/2}$ for the $Fe(dcb)_3^{2+/3+}$ couple is significantly more positive than that of $Co(DTB)_3^{2+/3+}$; consequently, iron(III) has more-than-sufficient oxidizing strength to oxidize cobalt(II), but iron(II) is thermodynamically too weak a reductant to reduce cobalt(III). Because the reaction of interest at the cathode in the DSSC is cobalt(III) reduction, the $Fe(dcb)_3^{2+/3+}$ couple is of no value in this regard. However, we have further determined that the catalysis of $Co(DTB)_3^{2+}$ oxidation by surface-bound, redox-active metal complexes is a relatively general phenomenon. It was therefore reasonable to believe that, given a metal complex with a sufficiently negative $E_{1/2}$, catalytic reduction of $Co(DTB)_3^{3+}$ would also be possible. On the basis of solution redox potentials, we first considered *cis*-dichloro-bis(4,4′-dicarboxylic acid-2.2′-bipridine)ruthenium(II). Unfortunately, when adsorbed to TCO substrates, the $E_{1/2}$ of this complex shifts to a potential that is too positive to reduce $Co(DTB)_3^{3+}$ efficiently. Because of its inherently more-negative solution $E_{1/2}$, the corresponding osmium(II) complex, *cis*-dichloro-bis(4,4′-dicarboxylic acid-2,2′-bipyridine)osmium(II), was synthesized and used to modify the TCO substrate electrodes. When adsorbed on TCO, the surface $E_{1/2}$ of $Os(dcb)_2Cl_2$ is ca. −310 mV versus ferrocene/ferrocenium, which is slightly negative of the potential for the $Co(DTB)_3^{2+/3+}$ couple. Consequently, these modified TCO electrodes proved to efficiently catalyze both the oxidation and reduction of $Co(DTB)_3^{2+/3+}$.

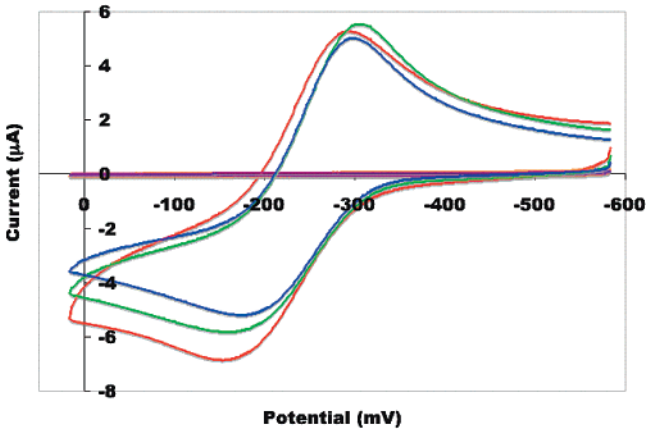

Figure 1. CVs of gold (red), FTO (brown), ITO (violet), $Os(dcb)_2Cl_2$-modified FTO (green), and $Os(dcb)_2Cl_2$-modified ITO (blue) working electrodes with ∼0.1 mM $Co(DTB)_3(ClO_4)_2$ in acetonitrile. The $Os(dcb)_2Cl_2$-modified electrodes give CVs nearly identical to gold, whereas unmodified TCO electrodes produce no current. Potentials are relative to ferrocene.

To more quantitatively evaluate the redox activity of $Os(dcb)_2Cl_2$-modified TCO electrodes, the CV behavior of $Co(DTB)_3^{2+}$ in solution was investigated. Working electrodes of vapor-deposited gold (i.e., the typical cathode used in $Co(DTB)_3^{2+/3+}$-mediated DSSCs), FTO and ITO (both $Os(dcb)_2Cl_2$-modified and unmodified), all patterned to the same shape and area, were compared, and the results are shown in Figure 1.

Essentially no current is observed on either unmodified ITO or FTO electrodes (Figure 1, brown and violet curves). In contrast, TCO electrodes that had been modified with $Os(dcb)_2Cl_2$ (Figure 1, blue and green curves) give voltammograms nearly identical to those obtained on gold (Figure 1, red curve). It must be noted that the cyclic voltammograms shown in Figure 1 are only quasi-reversible, evidenced by the magnitude of peak separation ($\Delta E_p \approx 140$ mV) and the broadness of the peaks. This is a result of the large

(17) Xue, D.; Elliott, C. M.; Gong, P.; Grainger, D. W.; Bignozzi, C. A.; Caramori, S. Indirect Electrochemical Sensing of DNA Hybridization Based on the Catalytic Oxidation of Cobalt(II). *J. Am. Chem. Soc.* **2007**, *129* (7), 1854−1855.

innersphere-reorganization energy typical of cobalt(II/III) redox processes.

Ideally, in a DSSC under illumination, there is negligible electron-transfer resistance at the cathode, and essentially all of the potential drop across the cell occurs at the photoanode.[18] On the basis of the results from the CVs in Figure 1, however, one would expect a large electron-transfer resistance in a photocell employing an unmodified TCO cathode and much-smaller resistance upon modification of the TCO cathode with $Os(dcb)_2Cl_2$. A three-electrode measurement, adapted from two previously reported procedures,[18,19] was devised to evaluate the cathode behavior. The cell bias was controlled externally while simultaneously monitoring the potential of the cathode and anode relative to the reference. This approach provides the photoanode potential (E_{an} vs ref), cathode potential (E_{cat} vs ref), cell potential ($E_{cell} = E_{cat} - E_{an}$), and current throughout a single scan.

The data from three cells employing different cathodes are shown in Figure 2. The horizontal axis for all of the plots is E_{cell}. Electrode potentials (E_{cat} and E_{an}) are plotted using the left vertical axis and are relative to the photocell's V_{oc}, determined by adjusting the reference potential slightly to account for the slight differences in V_{oc} commonly observed between the two photoanode halves (vide supra). Because of the difficulty of measuring the true illuminated area of the photoanode, cell current rather than the current density is also shown (right vertical axis). Part A of Figure 2 shows results for a cell incorporating an osmium-modified FTO cathode. The V_{oc} of the active cell corresponds to the E_{cell} at which no current flows (475 mV). At V_{oc}, there exists a large difference between E_{an} (essentially the quasi-Fermi energy of the FTO) and E_{cat} (the potential of which is determined by the mediator composition in solution). At short circuit, both electrodes are at the same potential ($E_{cell} = 0$), which is slightly negative of the mediator's reduction potential. This small magnitude of overpotential (~12 mV at short circuit) is characteristic of cathodes capable of efficiently reducing the redox mediator. Analogous results for a DSSC incorporating a gold cathode are shown in part B of Figure 2. With this cathode, no experimentally significant overpotential was required over the entire applied potential range, as evidenced by a perfectly constant E_{cat}. The situation is very different for an unmodified FTO cathode shown in part C of Figure 2. In this case, there is a very large potential drop needed at short circuit just to supply a very modest current. Clearly, both the current−voltage and electrode potential curves indicate that unmodified FTO is ill-suited as a cathode in DSSCs mediated by $Co(DTB)_3^{2+/3+}$.

Stacked Cells. UV−vis spectra of photoanodes with three different thicknesses of TiO_2 dyed with N3 are shown in Figure 3. These absorption spectra are qualitatively similar

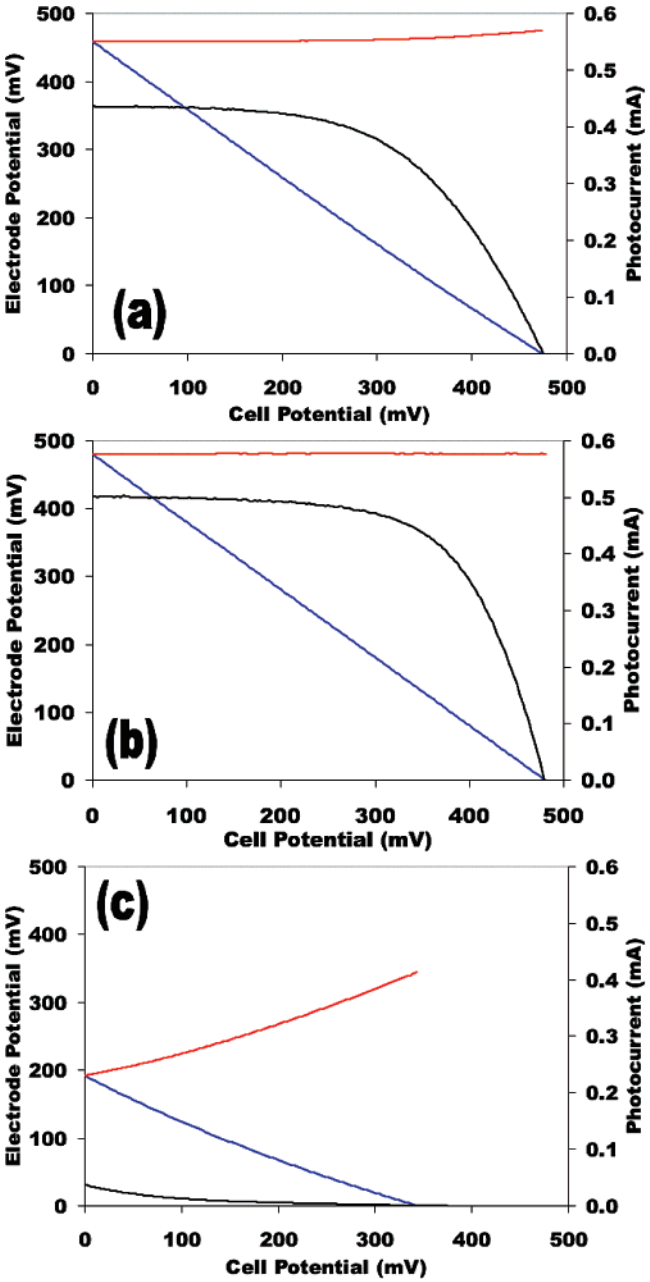

Figure 2. Results from three-electrode cell experiments with $Os(dcb)_2Cl_2$-modified FTO cathode (2a), gold cathode (2b), and unmodified FTO (2c). The black curves are current, the red curves are E_{cat}, and the blue curves are E_{an}.

to the solution spectrum of N3, exhibiting strong broad absorptions in the 400−550 nm region of the spectrum. As anticipated, the absorbance scales proportionately with the thickness of the TiO_2 layer. At longer wavelengths, N3 absorbs progressively less light until ca. 650 nm where little of the incident light is absorbed even for the thickest TiO_2 layer. In contrast to N3, the R8 cyanine dye has its maximum absorption at longer wavelengths. Figure 4 demonstrates the spectral complementarity of TiO_2 layers of similar thicknesses (ca. 2.4 μm) sensitized with the two dyes.

It is clear from Figure 4 that the R8 dye is a much stronger light absorber than the N3 dye. In fact, when free in dilute solution the molar extinction coefficient of the R8 dye is ca. 100 000 M^{-1} cm^{-1}.[5] It has been observed that when

(18) Zaban, A.; Zhang, J.; Diamant, Y.; Melemed, O.; Bisquert, J. Internal Reference Electrode in Dye Sensitized Solar Cells for Three-Electrode Electrochemical Characterizations. *J. Phys. Chem. B* **2003**, *107* (25), 6022−6025.

(19) Oskam, G.; Bergeron, B. V.; Meyer, G. J.; Searson, P. C. Pseudohalogens for Dye-Sensitized TiO_2 Photoelectrochemical Cells. *J. Phys. Chem. B* **2001**, *105* (29), 6867−6873.

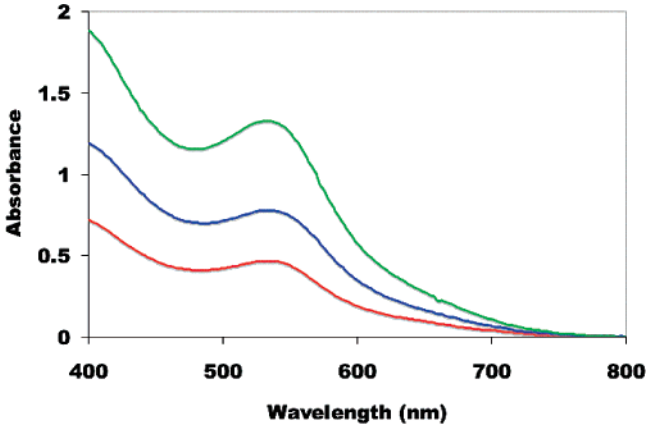

Figure 3. Visible absorption spectra of N3-dyed TiO_2. TiO_2 layers were 2.4 μm (red), 4.4 μm (blue), and 7.8 μm (green).

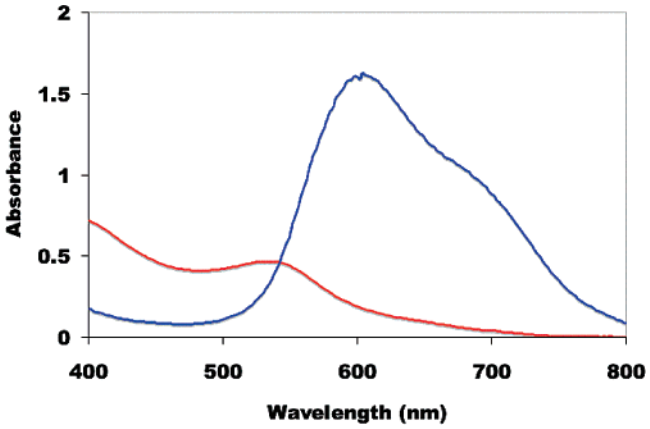

Figure 4. Visible absorption spectra of N3-dyed (red) and R8 dyed (blue) TiO_2. TiO_2 layers were 2.4 μm.

cyanine dyes aggregate into dimers their molar extinction coefficient is reduced by a factor of ca. 2.[20−22] Using the literature molar extinction coefficient value for the N3 dye of 14 200 M^{-1} cm^{-1},[13] and half of the literature value for the R8 dye, one calculates roughly equal surface concentrations of the two dyes. Even with the decreased molar extinction coefficient due to aggregation, the R8 dye is still a stronger light absorber than the N3 dye by a factor of ca. 3.5 times and absorbs in a region where the N3 dye does not.

To investigate the potential utility of an optically transparent DSSC cathode, two types of cells were prepared and examined. Each consisted of two individual cells wired in parallel and operated in optical tandem (i.e., stacked). The top, or front photoanode (closest to the source of illumination) is paired with an $Os(dcb)_2Cl_2$-modified FTO cathode. The second photoanode is paired with a conventional gold cathode.

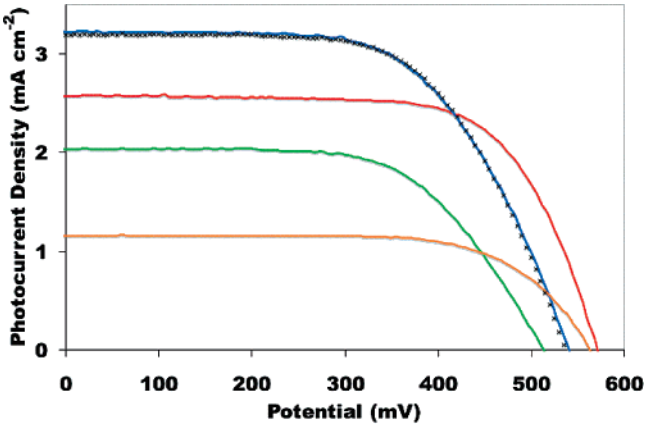

Figure 5. I−V curves for one-scotch cell (red), half-scotch stacked cell with both cells active (blue), front cell only (green), and back cell only (orange). Green and orange curves sum numerically (x's) to overlay the blue curve.

The first type of cell considered employs two N3-dyed photoanodes of the same thickness (half scotch, ca. 2.4 μm) stacked together. The performance of this cell was compared with a single photoanode of ca. twice the thickness (one scotch, ca. 4.4 μm) paired with a gold cathode. Current-voltage curves for these cells are shown in Figure 5.

Comparing the half-scotch stack (blue trace) with the one-scotch cell (red trace), the short-circuit current density, J_{sc}, of the half-scotch stack is 25% higher and the efficiency is 10% higher. Also shown in Figure 5 is how the front (green trace) and back (orange trace) cells in the half-scotch stack sum numerically to give the total output of the stack (x′s). The overall current densities of the stack are the sum of the current densities of the front and back cells at each potential. Similarly, as would be expected, the overall efficiency of the stack is the sum of the efficiencies for the front and back cells.

Because the absorbance of two half-scotch layers roughly adds up to the absorbance of a one-scotch layer (vide infra), it is reasonable to infer that the increase in current density of the stacked half-scotch cells results from a decrease in the number of photoinjected electrons in the TiO_2 that combine with the oxidized form of the mediator and with the photo-oxidized dye. The effect of both of these parasitic reactions is mitigated by decreasing the average time between charge-separation and charge-carrier collection. The decrease in overall V_{oc} of the half-scotch stack is due to the lower V_{oc} of the front cell. We have found over many experiments with cells employing $Co(DTB)_3^{2+/3+}$ as mediator that there is an inherent variability in behavior between photoanodes that are ostensibly identical or even between cells disassembled and reassembled with the same photoanode. In that context, the experimental variability in V_{oc} (ca. $\pm$ 60 mV) between the different photoanodes used to gather the data presented in Figure 5 is within typical limits. On the other hand, whereas identical cells often exhibit variability in the V_{oc}, the J_{sc} is typically more reproducible with a variability of ca. $\pm$ 0.2 mA cm^{-2}. Consequently the differences in J_{sc} and efficiency between the half-scotch stack and one-scotch cell are experimentally significant, even after accounting for the

(20) Lenhard, J. R.; Cameron, A. D. Electrochemistry and Electronic-Spectra of Cyanine Dye Radicals in Acetonitrile. *J. Phys. Chem.* **1993**, *97* (19), 4916−4925.
(21) Lenhard, J. R.; Parton, R. L. Electrochemical and Spectroscopic Analyses of the Thermodynamics of the Reversible Dimerization of Cyanine Radical Dications. *J. Am. Chem. Soc.* **1987**, *109* (19), 5808−5813.
(22) Parton, R. L.; Lenhard, J. R. Dimerization Reactions of Cyanine Radical Dications. *J. Org. Chem.* **1990**, *55* (1), 49−57.

ca. 9% difference in absorbance resulting from the small difference in total TiO_2 thickness.

The experiments giving rise to the data in Figure 5 demonstrate that $Os(dcb)_2Cl_2$-modified FTO can serve as a functional cathode in DSSCs mediated with $Co(DTB)_3^{2+/3+}$. Figure 3 demonstrates that a considerable amount of the long-wavelength portion of the visible solar spectrum will not be absorbed by N3 at any practical photoanode thickness. It is thus reasonable to consider a tandem cell incorporating a second dye that is spectrally complimentary to N3 such as R8 (cf. Figure 4).

Ehret and co-workers examined a collection of dicarboxylated cyanine dyes as TiO_2 sensitizers in I^-/I_3^--mediated DSSCs.[5] Some of these dyes were reported to produce photoanodes with electron-injection efficiencies comparable to N3. One dye in their study is structurally quite similar to R8. Unfortunately, that particular dye, which absorbs strongly in the red (hereafter the blue dye), gave only modest photocurrents and monochromatic conversion efficiencies (ca. 8%). Ehret and co-workers suggested that the poor injection efficiency likely results from dye aggregates on the surface that act as noninjecting traps.[5] This interpretation is consistent with our spectral results for the R8-dyed photoanodes, wherein the absorption maximum on TiO_2 (λ_{max} = 600 nm) is shifted relative to the dilute solution (λ_{max} = 660 nm). Also consistent with dye aggregation, the absorbance is less than expected for a simple adsorbed monolayer of individual dye molecules. Nevertheless, the R8 dye absorbs in a spectral region where photons are largely wasted with an N3-dyed photoanode. Ehret and co-workers also observed that there was an optimum thickness of ca. 4 μm for the dyed TiO_2 layer (with both the N3 dye and cyanine dyes), above which the short circuit photocurrent asymptotically approached a limiting value.[5] These observations suggest that some of the same issues (vide supra) involving loss of electrons from TiO_2/FTO to parasitic reactions are in play with cyanine-dyed photoanodes. Thus, potential advantages could accrue by considering tandem cells incorporating separate photoanodes dyed with N3 and R8 (i.e., in contrast to a single thicker photoanode incorporating both dyes).

The blue dye differs from R8 only in that the latter compound has one fewer methylene group in the alkyl chains of the carboxylic acid moieties. The presence of the carboxylic acid tail was reported to have only a minimal effect on both the absorption spectrum and redox potential (ca. 30 mV);[5] consequently, it is reasonable to assume that the R8 dye will be similar in these respects to the blue dye. Using their reported redox potential for the D/D^+ couple, there should be ample thermodynamic driving force for $Co(DTB)_3^{2+}$ to reduce photo-oxidized R8 (ca. 450 mV).[5] Moreover, their calculated potential for D^*/D^+ indicates electron photoinjection from R8* will occur.[5]

The fact that, relative to the blue dye, R8 has fewer methylene groups in the alkyl chain linking the cyanine and carboxylic acid moieties, could affect its coupling to the TiO_2 and thus the efficiency of charge injection. To evaluate R8 in this regard, photoaction spectra were obtained.

Figure 6 is a plot of incident photon to current efficiency versus wavelength for analogous cells, incorporating photoanodes dyed respectively with R8 and N3. On the basis of these data, R8 appears to exhibit similar electron-injection efficiency as the blue dye studied by Ehret, even with its shorter linkage.

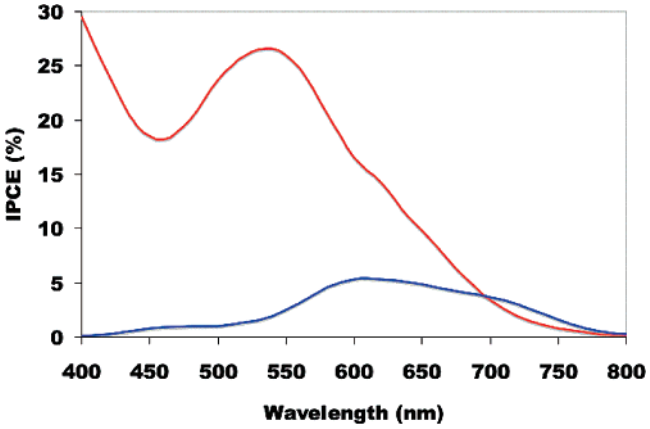

Figure 6. Photoaction spectra of operational DSSCs dyed with N3 (red) and R8 (blue). In both cells, $Co(DTB)_3^{2+/3+}$ was the redox mediator, and a gold cathode was used. TiO_2 layers were 2.4 μm.

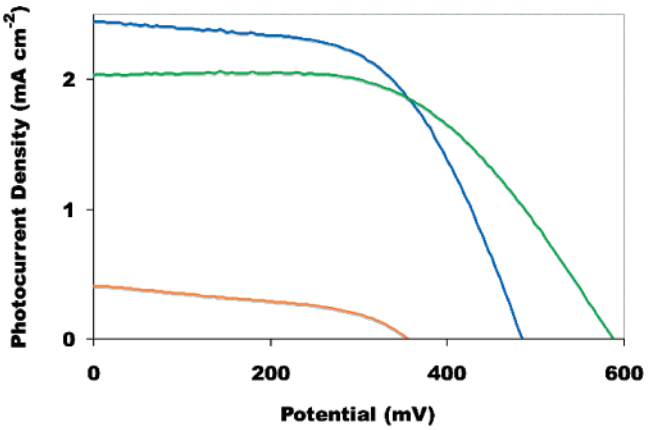

Figure 7. I−V curve for stacked cell employing half-scotch photoanodes (blue). Front cell (green) is N3-dyed photoanode with $Os(dcb)_2Cl_2$-modified FTO cathode, back cell (orange) is R8-dyed photoanode with gold cathode.

Despite its low photoelectron-injection efficiency, R8 does absorb photons in a wavelength range where N3 does not. A half-scotch stack where the front photoanode was sensitized with N3 and the back photoanode was sensitized with R8 was assembled and evaluated. The resulting current−voltage curves are shown in Figure 7.

The N3/R8 combination performed less well than the two-half-scotch N3 stack, yielding a V_{oc} of 485 mV, a J_{sc} of 2.44 mA cm^{-2}, and an efficiency of 0.67%. Additionally, the overall current-voltage curve was substantially nonideal in shape. All of these imperfections notwithstanding, the J_{sc} and overall power output of the tandem cell were greater than that of the front N3 cell alone, demonstrating proof of the concept. With a better performing sensitizer than R8, one could expect a substantial improvement in performance relative to cells having a single photoanode dyed with N3.

Conclusions

Whereas DSSCs have great potential as inexpensive alternatives to more-conventional solar conversion ap-

proaches, there are inherent issues with these cells that must be understood and there are problems to be overcome. The diffusive nature of charge-carrier transport in the solid phase for electrons and the liquid phase for holes makes the distance between charge collecting substrates a significant factor in the cell's performance. By employing electron-transfer mediator systems such as $Co(DTB)_3^{2+/3+}$, it becomes possible to investigate new options for addressing this issue that are unavailable with the I^-/I_3^- mediator system. We have found that, by proper chemical modification, transparent conducting metal-oxide electrodes can perform as transparent cathodes in $Co(DTB)_3^{2+/3+}$-mediated DSSCs. By employing these optically transparent cathodes and operating two cells in optical tandem, both the short-circuit current density and the overall cell efficiency can be increased. Relative to cells with a single thicker photoanode, the improved performance from stacked cells with two photoanodes dyed with the same dye likely arises from the shorter residence time of the electrons in the TiO_2 conduction band. When a second optically complimentary dye is employed with a second photoanode, a broader wavelength range of photon absorption can be realized.

Acknowledgment. Support of this work through a grant from the U.S. Department of Energy Office of Science (Grant DE-FG02-04ER15591) is acknowledged. Also, the authors wish to thank Professor Bruce A. Parkinson for providing us with samples of the cyanine dye.

Supporting Information Available: Detailed procedure for $TiCl_4$ treatment of photoanodes. SEM images of TiO_2, before and after $TiCl_4$ treatment. Current−voltage curves of operational $Co(DTB)_3^{2+/3}$-mediated DSSCs before and after $TiCl_4$ treatment. Cyclic voltammogram of unmodified FTO electrode and $Os(dcb)_2Cl_2$-modified FTO electrodes relative to $E_{1/2}$ of $Co(DTB)_3^{2+/3+}$. This material is available free of charge via the Internet at http://pubs.acs.org.

IC700709K